Supplementary material

Table S1 qPCR primer sequences used in this study.

Cxcl1	
Forward	5′-CTGGGATTCACCTCAAGAACATC-3′
Reverse	5′-CAGGGTCAAGGCAAGCCTC-3′
Cxcl2	
Forward	5′-CCAACCACCAGGCTACAGG-3′
Reverse	5′-GCGTCACACTCAAGCTCTG-3′
Cxcl5	
Forward	5′-TCCAGCTCGCCATTCATGC-3′
Reverse	5′-TTGCGGCTATGACTGAGGAAG-3′
Cxcl16	
Forward	5′-CCTTGTCTCTTGCGTTCTTCC-3′
Reverse	5′-TCCAAAGTACCCTGCGGTATC-3′
Irf1	
Forward	5′-ATGCCAATCACTCGAATGCG-3′
Reverse	5′-TTGTATCGGCCTGTGTGAATG-3′
Ifih1	
Forward	5′-AGATCAACACCTGTGGTAACACC-3′
Reverse	5′-CTCTAGGGCCTCCACGAACA-3′
Cdkn1a (P21)	
Forward	5′-CCTGGTGATGTCCGACCTG-3′
Reverse	5′-CCATGAGCGCATCGCAATC-3′
Gapdh	
Forward	5′-AGGTCGGTGTGAACGGATTTG-3′
Reverse	5′-TGTAGACCATGTAGTTGAGGTCA-3′

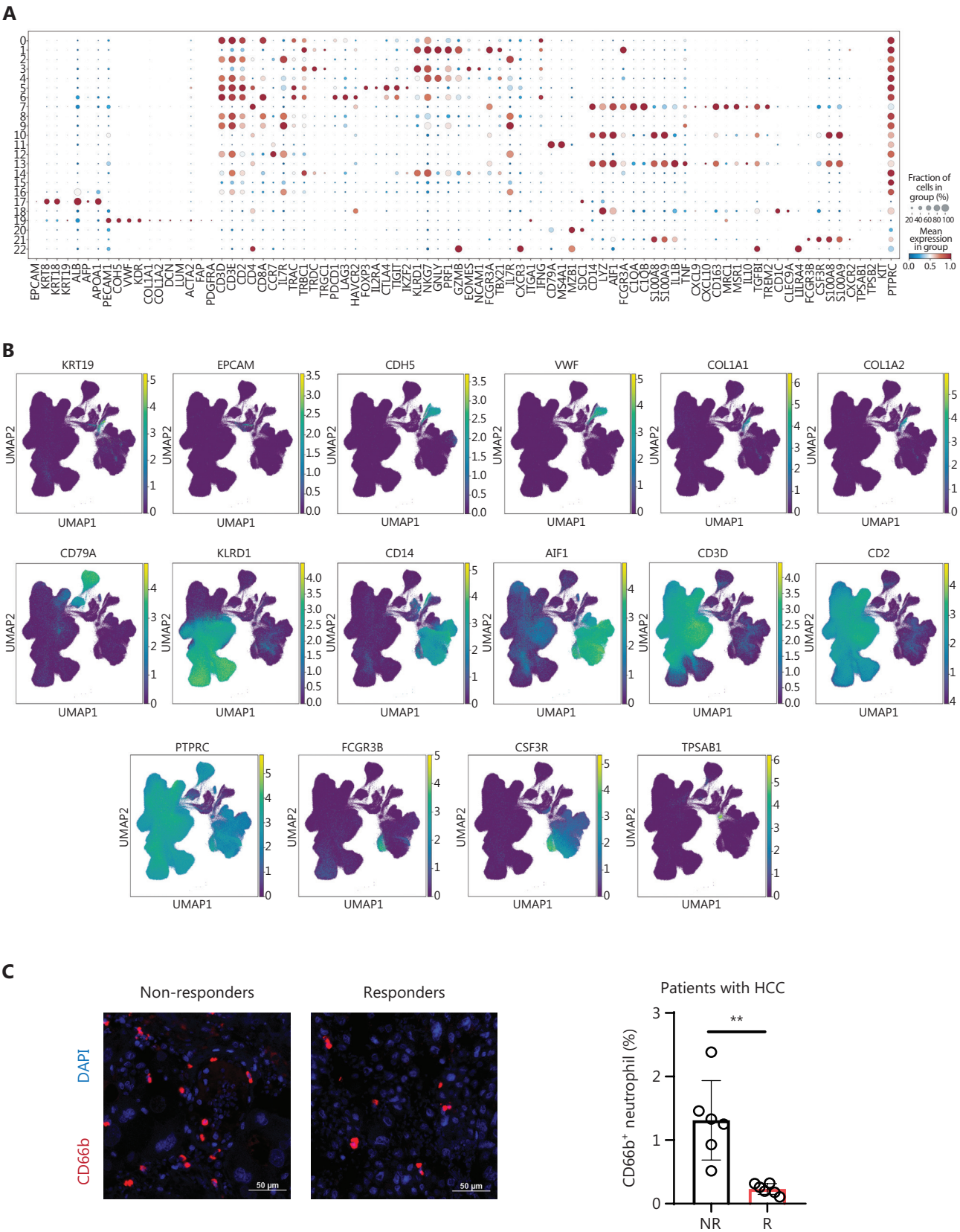

Figure S1 Continued

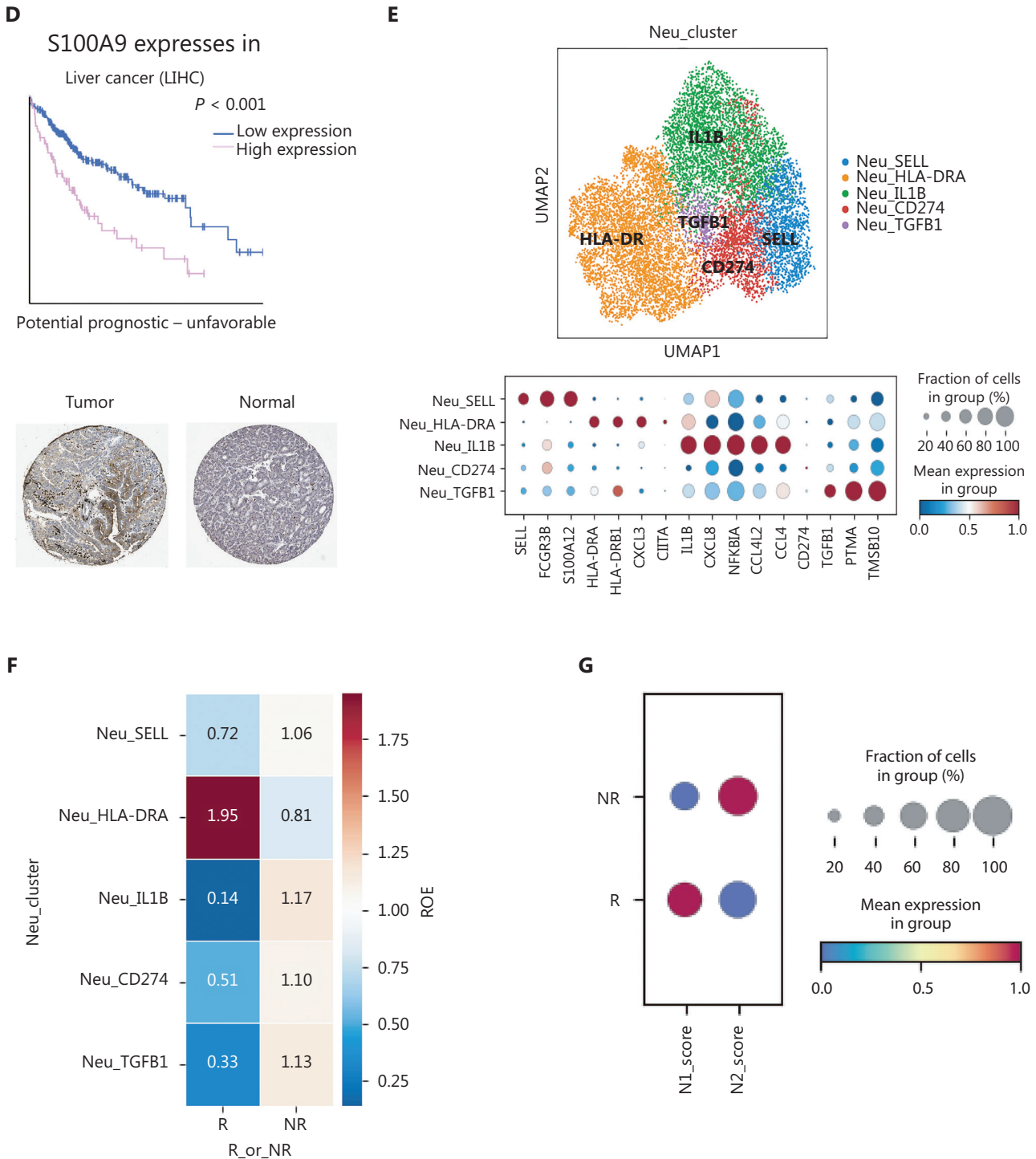

Figure S1 Single cell dimension reduction and clustering process. (A) Dot plots showing the expression levels of canonical marker genes used to annotate major cell clusters. (B) UMAP graphs showing distribution of the expression levels of selected marker genes. (C) mIHC assays of CD66b expression in human HCC clinical samples. (D). Expression of neutrophil marker S100A9 could serve as a prognostic marker in HCC (https://www.proteinatlas.org/ENSG00000163220-S100A9/cancer). (E) Sub-clustering of neutrophil populations based on signature markers. (F) Ro/e scores for neutrophil subclusters in responders and non-responders. (G) N1 and N2 scores for neutrophils in HCC samples from responders and non-responders.

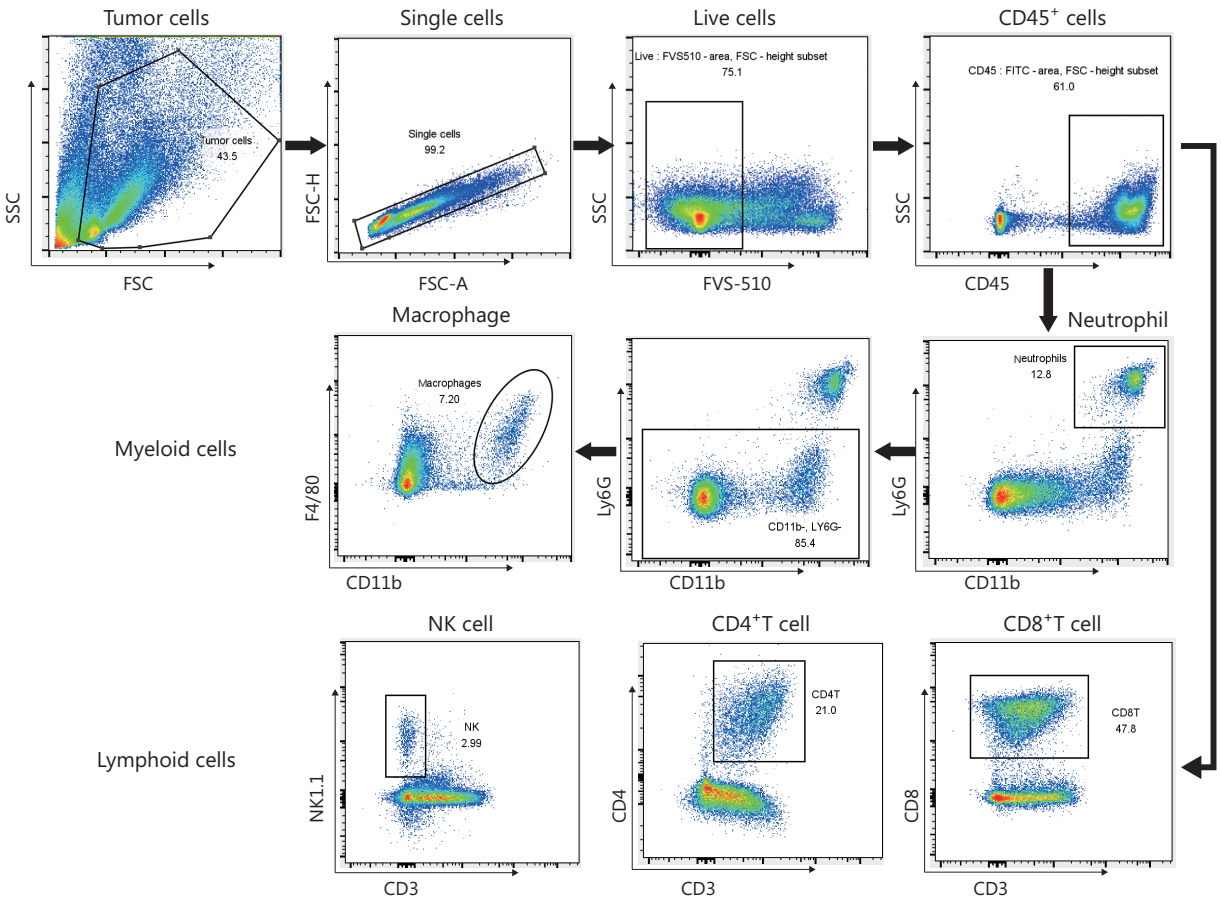

Figure S2 Flow cytometry gating strategy. The sequential gating hierarchy is shown for identifying tumor infiltration neutrophils ($CD11b^+$ $Ly6g^+$), macrophages ($Ly6g^-$ $CD11b^+$ $F4/80^+$), $CD8^+$ T cells ($CD3^+$ $CD8^+$), $CD4^+$ T cells ($CD3^+$ $CD4^+$), and NK cells ($CD3^-$ $NK1.1^+$) from live $CD45^+$ leukocytes ($FVS510^-$).

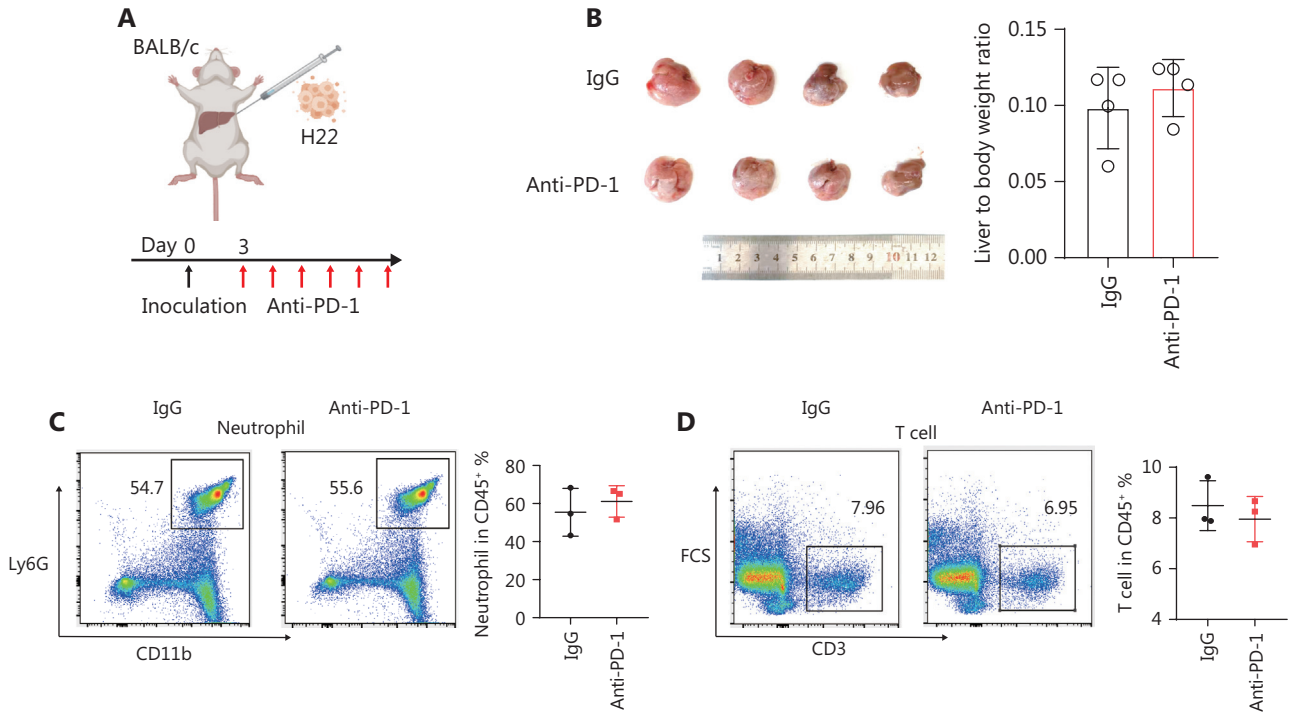

Figure S3 H22 ICI-resistant model with anti-PD-1 treatments. (A) Flowchart showing the H22 model with treatments (n = 4 per group). (B) Tumor sizes for different groups in H22 models. (C, D) Flow cytometric analysis of TANs (C) and tumor-infiltrating T cells (D) in the TME of H22 tumors.

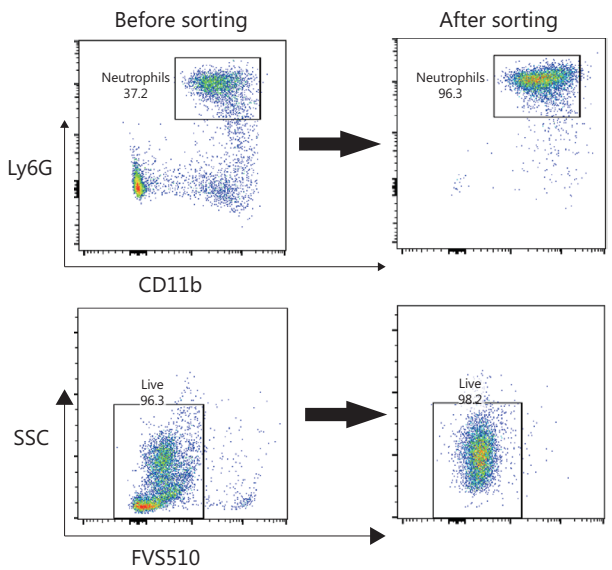

Figure S4 Purity and viability of isolated neutrophils before and after enrichment.

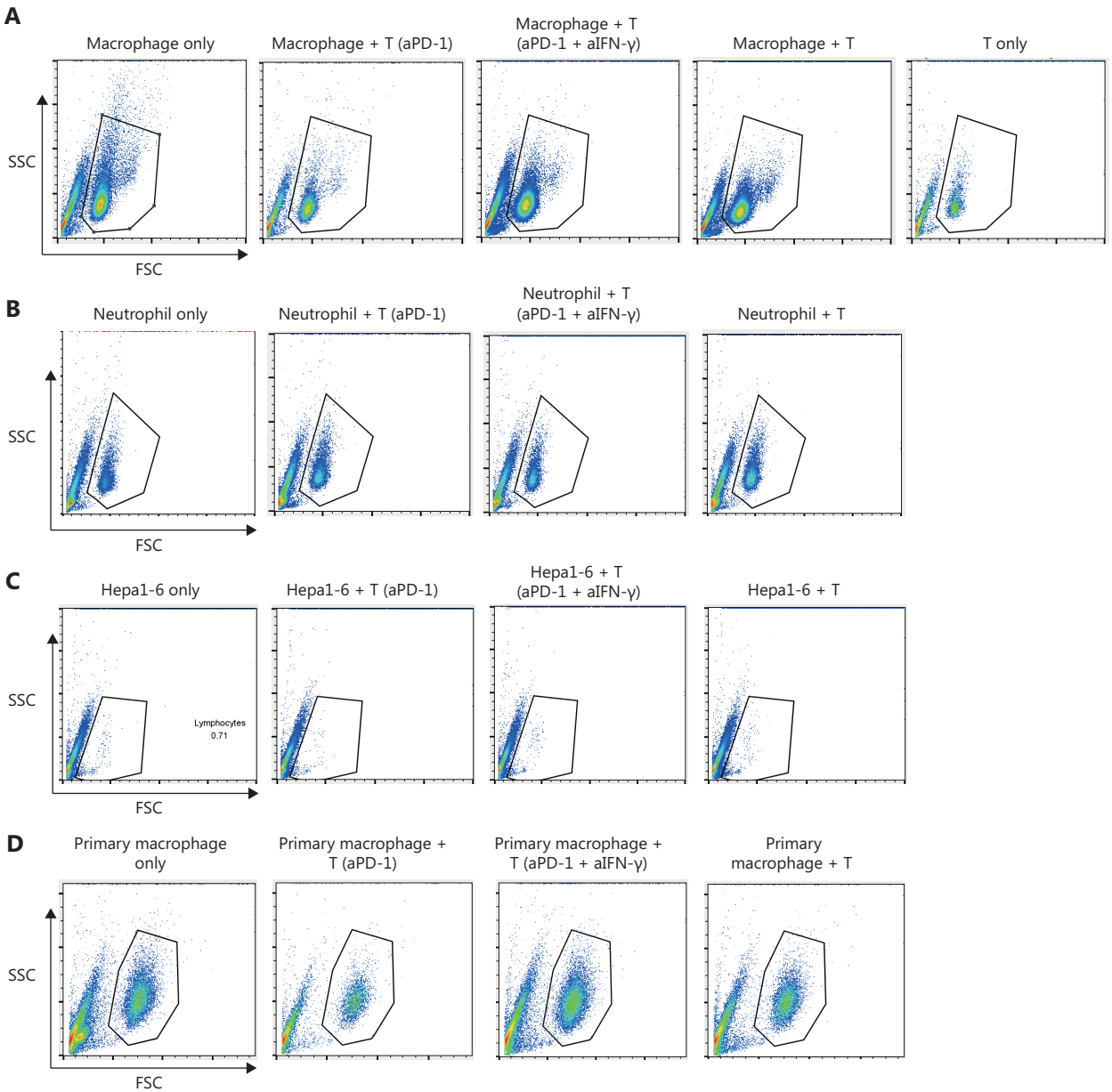

Figure S5 Cell counts for migrating neutrophils mediated by different cells. Accurate cell counts were obtained for migrating neutrophils in the lower chamber using flow cytometry. (A) Neutrophil migration mediated by macrophages under different T cell treatments. (B) Neutrophil migration mediated by neutrophils under different T cell treatments. (C) Neutrophil migration mediated by Hep1-6 cells under different T cell treatments. (D) Neutrophil migration mediated by primary macrophages under different T cell treatments. Experiments were performed with three independent biological replicates.

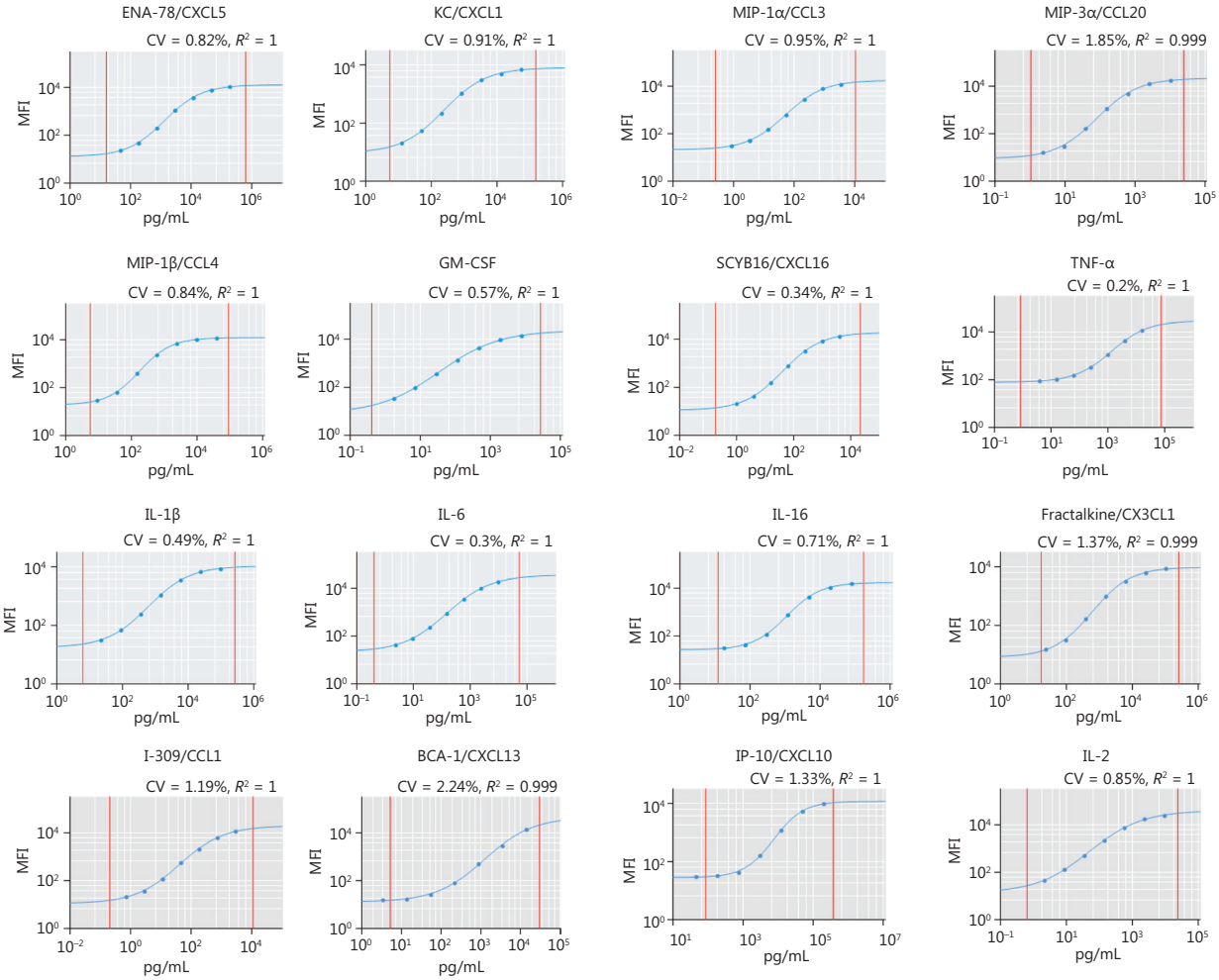

Figure S6 Continued

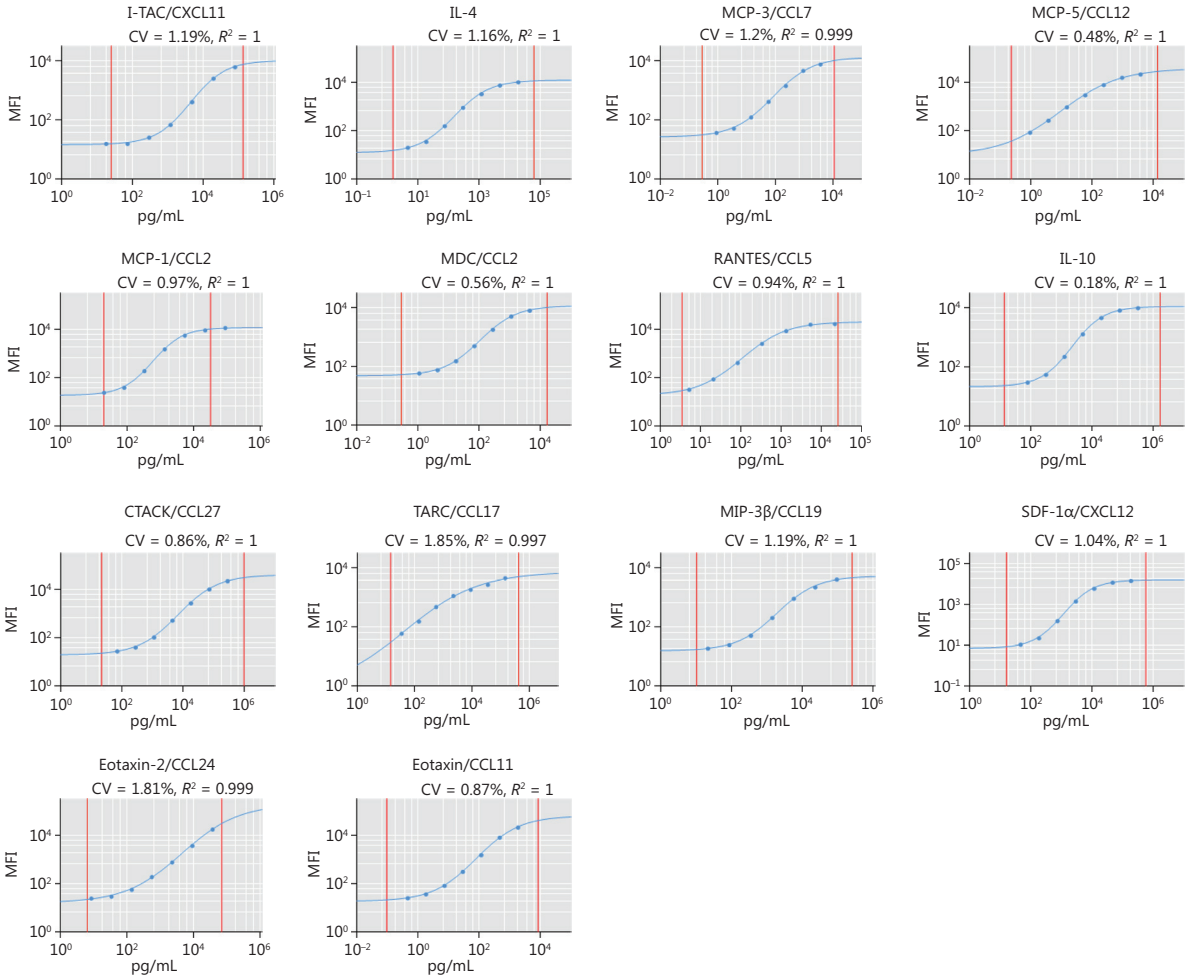

Figure S6 Standard curves for multiple Luminex ELISA assays. Standard curves are shown for the chemokines evaluated in this study. R^2 > 0.99 for all curves, confirming the validity of the quantitative measurements.